Research in Pharmaceutical Sciences, April 2026; 21(2): 164-177
Received: 20-11-2024
Peer Reviewed: 20-02-2025
Revised: 22-04-2025
Accepted: 28-04-2025
Published: 24-04-2026

School of Pharmacy & Pharmaceutical Sciences
Isfahan University of Medical Sciences

Original Article

GPR97 variants and their influence on pathological myopia: implications for glucocorticoid treatment

Qi Zhao[1], Zhaoxia Mu[1], Huihui Gu[1], Wei Cheng[1], Yulian Xu[1], Yingying Jiang[1], Geping Wu[2], and Lijun Pu[1,*]

[1]*Department of Ophthalmology, Zhangjiagang Hospital Affiliated to Soochow University, Suzhou, Jiangsu, China.*
[2]*Institute of Translational Medicine, Zhangjiagang Hospital Affiliated to Soochow University, Suzhou, Jiangsu, China.*

Abstract

Background and purpose: Pathologic myopia (PM) is a severe form of myopia associated with structural changes in the eye, leading to vision impairment. Identifying genetic factors that contribute to PM can enhance the treatment of the condition. This study aimed to investigate the association between the *GPR97* and PM and to evaluate the impact of glucocorticoid treatment on PM.

Experimental approach: A cohort of 412 sporadic PM patients underwent Sanger sequencing and genotyping for GPR97 gene variants. Thirty-one PM patients with various GPR97 genotypes received glucocorticoid and brinzolamide treatment over 24 months. Real-time PCR was employed to examine the target gene mRNA expression. A scratch assay was performed to detect cell migration ability.

Findings/Results: A significant association was identified between GPR97 rs76688596 genotypes and PM occurrence. The CC genotype was linked to elevated intraocular pressure (IOP). In human scleral fibroblasts, overexpression of GPR97 Arg396 resulted in upregulation of IOP-related genes serine/arginine-rich splicing factor 3, peptidyl-prolyl cis-trans isomerase 4, peptidyl-prolyl cis-trans isomerase 5, and nuclear receptor subfamily 3 group C member 1. The GPR97 Arg396 mutation inhibited the glucocorticoid-GPR97 axis and reduced cell migration ability. Clinically, CC genotype carriers exhibited significant improvements in axial length, spherical equivalent, IOP, best-corrected visual acuity, and visual field mean sensitivity with glucocorticoid treatment.

Conclusion and implications: The study revealed that the GPR97 rs76688596 G > C variant is associated with PM pathogenesis, influencing gene expression related to IOP. The differential response to glucocorticoid treatment among GPR97 genotypes suggests personalized therapeutic potential.

Keywords: Glucocorticoid treatment; GPR97; Intraocular pressure; Pathologic myopia.

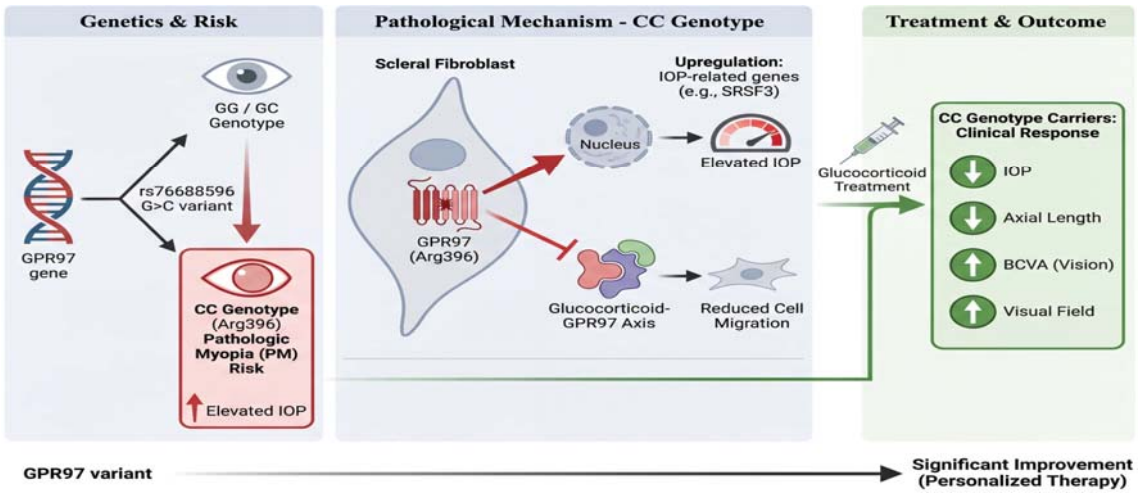

*Corresponding authors: L. Pu
Tel: +86-13962259830, Fax: +86-512-56919800
Email: PLJ0237@suda.edu.cn

Access this article online
Website: http://rps.mui.ac.ir
DOI: 10.4103/RPS.RPS_217_24

INTRODUCTION

Pathologic myopia (PM), a leading cause of low vision and blindness worldwide, primarily occurs in eyes with high myopia. Epidemiological studies highlight the significant social and economic burden of this condition. Its global prevalence ranges from 0.2% to 8.4% (1), with a rate of 0.95% in China (2). The heritability of axial length (AL) is substantial, ranging from 40% to 94% (3), emphasizing the significant role of genetics in the development of PM. Several genes, including *MYP1* (4), *LAMA1* (5), and Optoglycan (6), have been implicated in PM pathogenesis. Despite these findings, the genetic basis of myopia-related refractive errors remains incompletely understood, necessitating further investigations across diverse populations and environmental contexts. G protein-coupled receptors (GPCRs), such as *LGR4* (7), dopamine receptors, melatonin receptors *MT1* or *MT2* (8), *GPR58* (9), and *GPR143* (10-12), have been linked to eyeball development and ophthalmic conditions. GPR97, also known as adhesion G protein-coupled receptor G3 (*ADGRG3*), is a member of the orphan adhesion GPCR family. Recent work by Ping *et al*. (10) using single-particle cryo-electron microscopy has shed light on the complexes formed by GPR97 activation in response to exogenous ligand beclomethasone and endogenous ligand hydrocortisone. The unique glucocorticoid binding to GPR97, facilitated by hydrophobic interactions and hydrogen bonding, reveals a distinctive activation mechanism, differing from other GPCR family receptors due to the absence of conserved motifs (10). This activation leads to downstream G protein signaling *via* the HLY motif, affecting key cellular processes such as cytoskeletal rearrangement, cell adhesion, and migration by regulating small GTPases (11). Additionally, G(o) protein palmitoylation enhances the interaction between GPR97 and G(o), stabilizing the ligand-binding cavity within GPR97 (12). Despite its association with cell adhesion, migration, and cytoskeletal rearrangement, particularly in endothelial cells (11). The physiological role and regulatory mechanism of GPR97 in the visual epithelium remain to be elucidated.

PM is a progressive ocular disorder characterized by excessive AL growth, leading to structural changes in the eye such as retinal thinning, choroidal atrophy, and scleral remodeling, all of which contribute to severe visual impairment (13). The relentless elongation of the AL, a hallmark of PM, is intricately linked to changes in refractive error. Glucocorticoids, hormones secreted by the adrenal cortex, play a pivotal role in regulating gene expression by binding to glucocorticoid receptors, yet their prolonged use comes with severe risks, including intraocular hypertension, glaucoma, and cataracts (14-17). These adverse outcomes are driven by increased resistance in aqueous humor drainage pathways, with genetic factors such as MYOC and IGFBP2 influencing individual responses to glucocorticoid-induced intraocular pressure (IOP) elevation. The morphological changes associated with high myopia, including lacquer cracks and choroidal neovascularization, are further complicated by scleral remodeling, which heightens susceptibility to glaucoma. Recent findings linking the glucocorticoid-GPR97-binding complex to both PM and primary open-angle glaucoma highlight the shared genetic underpinnings between the two conditions (10). With evidence suggesting that genetic variations, particularly in the GPR97 gene, may modulate glucocorticoid responses, this study explores the potential influence of GPR97 polymorphisms on PM susceptibility and treatment outcomes. We hypothesize that specific single-nucleotide polymorphisms (SNPs) in PM susceptibility genes may modulate glucocorticoid response, thereby offering insights into personalized treatment strategies for PM. By investigating how these genetic differences impact myopia progression in response to glucocorticoid treatment, we aim to uncover personalized therapeutic strategies for PM, paving the way for more effective, tailored interventions.

MATERIALS AND METHODS

Subjects

A total of 412 patients diagnosed with PM were recruited from the Department of Ophthalmology at Zhangjiagang Hospital. Clinical and demographic data are detailed in Table S1. Among the PM patients, there were

201 males and 211 females, with an average age of 29.3 ± 3.5 years. All selected patients had binocular disease, with atrophy and degeneration of the macular region in both eyes. The right eye had a spherical equivalent (SE) of -10.8 ± (-1.54) diopters (D), and the left eye had -10.71 ± (-2.12) D, with no statistical difference between eyes (paired t-test, t = -1.214, P = 0.136). The average AL of the right eye was 29.39 ± 3.03 mm, and the left eye was 29.33 ± 2.64 mm, with no statistical difference between eyes (paired t-test, t = 1.214, P = 0.138). Exclusion of PM patients with other ocular comorbidities. Exclusion of patients with autoimmune diseases from the PM patients. The control group consisted of 269 healthy individuals from Zhangjiagang Hospital undergoing physical examination, excluding those with eye diseases. Both the case and control groups were unrelated Chinese Han populations. The study protocol received approval from the Research Committee of Zhangjiagang Hospital Affiliated to Soochow University, Suzhou, Jiangsu, China, with approval number IRB#: 2019-ZJG1703. All procedures adhered to the principles of the Declaration of Helsinki, and written informed consent was obtained from all participants or their parent/legal guardian/next of kin before study participation.

Genotyping

A total of 5 mL of venous whole blood was collected in EDTA-containing blood tubes and stored at -20 °C. Genomic DNA extraction from peripheral blood was performed using the Qiagen DNA extraction kit, and DNA concentration was assessed using NanoDrop 2000. The extracted DNA samples were stored at -20 °C until further processing. Polymerase chain reaction (PCR) and Sanger sequencing were carried out for the GPR97 gene and SNPs obtained from dbSNP. Primers were synthesized by Ruibiotech Co., Ltd. (Beijing, China). The sequences for genotyping primers can be found (Table S2). Sequencing covered the GPR97 promoter region and 12 exons, and Sanger sequencing was conducted using an ABI3130XL genetic analyzer. The experimental results were analyzed using the Chromas program 2.6.6 (Technelysium Pty Ltd).

Bioinformatics analyses

The pathogenicity of the mutation site was predicted and analyzed using PolyPhen-2, SIFT and MutationTaster. Bioinformatics analyses were conducted using the PolyPhen-2 (http://genetics.bwh.harvard.edu/pph2/), SIFT (http://sift.jcvi.org/), and MutationTaster (http://www.mutationtaster.org/) platforms to predict the pathogenicity of mutation sites. In the case of MutationTaster, a higher score approaching 1 indicates greater reliability of the prediction. PolyPhen-2 assigns prediction values ranging from 0 (likely benign) to 1 (likely harmful), while SIFT prediction values range from 0 to 1. A SIFT prediction value ≤ 0.05 suggests detrimental amino acid substitution, whereas a value > 0.05 suggests tolerance. The transmembrane structure of GPR97 was predicted using TOPCONS, a web server that integrates membrane protein topology and signal peptide prediction (https://topcons.cbr.su.se/).

Primary sclera fibroblast culture

Methods for the isolation and culture of scleral peripapillary fibroblasts have been previously described (18). Briefly, donor eyes were acquired from the Department of Ophthalmology at Zhangjiagang Hospital within 24 h postmortem, with consent obtained for research use. None of the donors had a history of ocular disease after clinical examination. A 2-mm-wide circular band of sclera surrounding the optic nerve head, known as the peripapillary sclera, was carefully dissected from the donor eyes and digested overnight with collagenase (Serva, Heidelberg, Germany) at 37 °C. The digested tissue was then filtered through a 70 μm filter (Falcon; BD, Franklin Lakes, NJ) and resuspended. The resulting human scleral fibroblasts (HSFs) were cultured in Dulbecco's modified Eagle's medium (DMEM; Gibco, Grand Island, NY) supplemented with 20% fetal bovine serum (FBS) and 1% penicillin-streptomycin (Hyclone, South Logan, UT) at 37 °C in a 5% CO_2 atmosphere. After one week, the medium was replaced every three days. HSFs from passage 1 were subsequently cultured in DMEM with 15% FBS and 1% penicillin-streptomycin. All experiments were conducted

on HSFs between passages 4 and 7. The GPR97 cDNA clone was obtained from Genescript. Site mutation was performed according to the instructions of the Phusion Site-Directed Mutagenesis kit (Thermo Fisher, USA). HSF cells were transfected with GPR97 wild-type (WT) and Arg396 mutated genes using liposome transfection reagent (Lipofectamine 3,000, USA). Cells were stimulated with cortisone (16 nM, Solarbio, Beijing) for 24 h, and the total RNA was collected to analyze the expression of *GPR97* downstream genes.

Real-time PCR

Total RNA was extracted following the standard procedure of Trizol reagent (Thermo Fisher, USA). The RNA quality and quantity were assessed by Qubit using the Qubit RNA HS assay kit (Thermo Fisher). The reverse transcription reaction (5 μg total RNA/RT reaction) was carried out with incubation at 25 °C for 10 min, 42 °C for 50 min, followed by 70 °C for 15 min using SuperScript II reverse transcriptase with random hexamers (Thermo Fisher, USA) and the obtained cDNA was subjected to real-time PCR (RT-PCR) on QuantStudio 3 Real-Time PCR machine (Applied Biosystems, USA). RT-PCR assay consisted of 12.5 μL of PowerUp SYBR Green Master Mix (×2) (Thermo Fisher, USA), 0.3 μM of each primer (forward and reverse), 3 μL of template, and DNA/nuclease-free water up to a volume of 25 μL. Negative template control consisted of DNA/nuclease-free water as template. All reactions were run in triplicate. The amplification was achieved by an initial denaturation time of 3 min at 95 °C, 40 cycles of 95 °C for 15 s, and 60 °C for 1 min. A dissociation melting curve was performed after amplification by a gradual rise in temperature from 65 to 95 °C, with fluorescence signal measurement every 0.5 °C. Melting curve analysis was done to assess the quality of the final PCR products. The threshold cycle Ct values were calculated by fixing the basal fluorescence at 0.05 units. The average Ct value was calculated. The ΔCt values were calculated as Ct_{sample} - $Ct_{\beta\text{-}actin}$. The N-fold increase or decrease in expression was calculated via the $2^{-\Delta\Delta Ct}$ method using the Ct β-actin value as the reference point. The quantitative values for target gene expression were then normalized and compared to the control group. The primer sequences applied for COL1A1, COL2A1, SRSF3, FKBP4, FKBP5, NR3C1, N-Cadherin, Fibronectin, and β-actin can be found in Table S3.

Immunofluorescence

Immunofluorescence was performed using a standard protocol to measure the disassembly of actin stress fibres by detecting phalloidin-FITC (1:200, #P5282, MilliporeSigma, St Louis, MO) and N-cadherin (1:100, #ab93525, Abcam) in fixed cells. The staining was visualized using a Leica TCS SL Confocal Microscope (Deerfield, IL, US).

Scratch assay to detect cell migration ability

The treated HSF cells were seeded in 3 mL of the inner well of a 6-well plate. After the cells reached 90% confluence, a 200 μL pipette tip was used to vertically scratch the plate, and PBS was used to wash 3 times. Afterwards, the HSF cells were divided into 3 groups (empty control group, GPR97 WT, and GPR97 Gly396), and continued to be cultured. The width of the scratch wound was observed and recorded under an optical microscope at 0 h and 24 h of the experiment, respectively, and the wound healing rate was calculated as the basis for judging the cell migration ability according to the equation below:

$$\text{Wound healing ratio (\%)} = \frac{\text{Initial wound width} - \text{wound width (24 h)}}{\text{Initial wound width}} \times 100$$

Treatment design

A total of 31 patients with PM consented and were included in the treatment cohorts at our center. The remaining 381 patients did not provide consent and were therefore excluded from the treatment study. Confirmation of patients was achieved through fluorescein fundus angiography (FFA) examination. The cohort comprised 16 males and 15 females, aged between 34 and 41 years, with an average age of 37.5 ± 7.8 years. Among them, 12 patients carried the GPR97 rs76688596 GG genotype, 13 carried the GPR97 rs76688596 GC genotype, and 6 carried the GPR97 rs76688596 CC genotype. Inclusion criteria encompassed complaints of flashes, photophobia, and fixed shadow symptoms in

both eyes, with myopia increasing by more than 0.50 D/year within the past 2-10 years. Additional criteria included AL ≥ 27.5 mm, SE ≤ -6.00 D, and IOP between 17.5-21.5 mmHg. Treatment involved oral moderate-dose glucocorticoid prednisone acetate tablets (Shandong Xinhua Pharmaceutical Co., Ltd.) at an initial dose of 0.75 mg/kg/day. Dosage adjustments were made based on the patient's response, with a gradual reduction of 10 mg every 2 weeks in stable or improving conditions. In case of symptom recurrence, the original dosage was maintained for 2 weeks. The average treatment duration was 13.5 weeks.

Observation indicators

Clinic follow-up visits were scheduled at 1, 3, 6, 12, 18, and 24 months following the initiation of treatment. During these visits, clinical symptoms were meticulously recorded, and various measurements were taken, including AL, SE, IOP, best-corrected visual acuity (BCVA), and mean sensitivity (MS) of visual fields. A comprehensive refractometer (Topcon, Japan) was used to measure SE consistently. BCVA was assessed using an internationally standardized visual acuity chart, with the results converted to LogMAR visual acuity for statistical analysis. AL was measured using a biometric measurement device, while visual field MS values were recorded using the Zeiss Humphrey Visual Field Analyzer 750i with the 30-2 program, targeting the central 30° visual field. To ensure reliability, the examined eye underwent two checks with a 10-min break in between, and the results of the second check were used for analysis to mitigate the impact of learning effects on visual field results. IOP was measured using the Goldmann Applanation Tonometry. Each measurement comprised three consecutive readings, with a difference of less than or equal to 3 mmHg.

Statistical analysis

We tested whether the population is in the Hardy-Weinberg equilibrium (HWE) or not. The HWE test was applied to 9 SNPs of the GPR97 gene. The chi-square test was used to compare the differences in genotype distribution and allele frequency between case and control groups. Adjusted *P*-values were corrected for multiple testing using the Bonferroni test. Data analysis was performed using SPSS 22.0 software. Variance analysis of repeated measurements was employed for data at multiple time points. Pearson's method was used for correlation analysis. *P*-values < 0.05 were considered statistically significant.

RESULTS

Association of GPR97 polymorphisms with PM

We screened the SNPs in the GPR97 promoter, exons, and adjacent introns by direct sequencing in 25 healthy controls and found 9 SNPs (rs9927721, rs8045257, rs56288453, rs62039891, rs9930732, rs73552781, rs76894559, rs76688596, and rs1064328; with frequency of more than 1%), all of which are already registered in the dbSNP. Results indicated that the genotype distribution aligned with the HWE ($P > 0.05$, Table S4). Analyzing the allele distribution of these SNPs in 412 PM patients and 269 healthy controls using the chi-square test, after Bonferroni correction, no significant difference in genotype and allele frequency was observed for rs9927721, rs8045257, rs56288453, rs62039891, rs9930732, rs73552781, rs76894559, and rs1064328 SNPs between PM and healthy controls ($P > 0.05$). However, a significant difference was noted in the genotype G/G, G/C, C/C of rs76688596 ($P = 0.006$, adjusted $P = 0.05$, OR = 1.95 (0.99-3.38), (Table 1), and in the alleles G and C ($P = 0.004$, adjusted $P = 0.032$, OR = 2.035(1.09-3.69), Table 1) between the case and control groups. The recorded dbSNP rs76688596 G > A exhibited a G > C substitution in our cohort study, indicating a potential variation specific to distinct population and ethnic groups. Additionally, the genotype changes at this locus resulted in a variation in the encoded GPR97 protein (Gly396Arg, G > R), which was predicted to be located in the transmembrane domain 4 by TOPCONS. Results showed that SIFT, PolyPhen-2, and MutationTaster were all predicted to be harmful (PolyPhen-2 score = 0.819; SIFT score = 0.053; MutationTaster score = 1).

Table 1. The frequency of SNP locus genotypes and alleles between high myopia and healthy controls.

Gene polymorphism	Genotype frequencies			Allele frequencies	
rs9927721, A > C	**AA**	**AC**	**CC**	**A**	**C**
PM patients (n = 412)	343 (83.252%)	63 (15.291%)	6 (1.456%)	375 (91.019%)	37 (8.981%)
Controls (n = 269)	238 (88.476%)	31 (11.524%)	0 (0.0%)	254 (94.424%)	15 (5.576%)
Statistics	*P* value*: 0.839			*P* value*: 0.914	
				OR (95% CI): 1.65 (0.89-3.12)	
rs8045257, G > A	**GG**	**GA**	**AA**	**G**	**A**
PM patients (n = 412)	332 (80.583%)	75 (18.204%)	5 (1.214%)	370 (89.806%)	42 (10.194%)
Controls (n = 269)	236 (87.732%)	33 (12.268%)	0 (0.0%)	252 (93.68%)	17 (6.32%)
Statistics	*P* value*: 0.857			*P* value*: 0.774	
				OR (95% CI): 1.75 (0.97-3.18)	
rs56288453, C > T	**CC**	**CT**	**TT**	**C**	**T**
PM patients (n = 412)	401 (97.33%)	9 (2.184%)	2 (0.485%)	406 (98.544%)	6 (1.456%)
Controls (n = 269)	262 (97.398%)	2 (0.743%)	5 (1.859%)	264 (98.141%)	5 (1.859%)
Statistics	*P* value*: 0.954			*P* value*: 0.994	
				OR (95% CI): 0.64 (0.23-1.89)	
rs62039891, G > T	**GG**	**GA**	**AA**	**G**	**A**
PM patients (n = 412)	301 (73.058%)	102 (24.757%)	9 (2.184%)	351 (85.194%)	61 (14.806%)
Controls (n = 269)	205 (76.208%)	64 (23.792%)	0 (0.0%)	237 (88.104%)	32 (11.896%)
Statistics	*P* value*: 0.921			*P* value*: 0.423	
				OR (95% CI): 1.28 (0.81-2.01)	
rs9930732, C > T	**CC**	**CT**	**TT**	**C**	**T**
PM patients (n = 412)	208 (50.485%)	156 (37.864%)	48 (11.65%)	286 (69.417%)	126 (30.583%)
Controls (n = 269)	160 (59.48%)	92 (34.201%)	17 (6.32%)	206 (76.58%)	63 (23.42%)
Statistics	*P* value*: 0.877			*P* value*: 0.761	
				OR (95% CI): 1.45 (1.03-2.05)	
rs73552781, C > T	**CC**	**CT**	**TT**	**C**	**T**
PM patients (n = 412)	122 (29.612%)	180 (43.689%)	110 (26.699%)	212 (51.456%)	200 (48.544%)
Controls (n = 269)	66 (24.535%)	139 (51.673%)	64 (23.792%)	136 (50.558%)	133 (49.442%)
Statistics	*P* value*: 0.934			*P* value*: 0.991	
				OR (95% CI): 0.96 (0.71-1.31)	
rs76894559, C > T	**CC**	**CT**	**TT**	**C**	**T**
PM patients (n = 412)	124 (30.097%)	197 (47.816%)	91 (22.087%)	222 (53.883%)	190 (46.117%)
Controls (n = 269)	104 (38.662%)	125 (46.468%)	10 (3.717%)	166 (61.71%)	103 (38.29%)
Statistics	*P* value*: 0.947			*P* value*: 0.459	
				OR (95% CI): 1.38 (1.01-1.98)	
rs76688596, G > C	**GG**	**GC**	**CC**	**G**	**C**
PM patients (n = 412)	342 (83.01%)	64 (15.534%)	6 (1.456%)	374 (90.777%)	38 (9.223%)
Controls (n = 269)	247 (91.822%)	12 (4.461%)	0 (0.0%)	263 (97.77%)	6 (2.23%)
Statistics	*P* value*: 0.054			*P* value*: 0.036	
				OR (95% CI): 2.03 (1.09-3.69)	
rs1064328, A > G	**AA**	**AG**	**GG**	**A**	**G**
PM patients (n = 412)	160 (38.835%)	191 (46.359%)	61 (14.806%)	255 (61.893%)	157 (38.107%)
Controls (n = 269)	90 (33.457%)	113 (42.007%)	66 (24.535%)	146 (54.275%)	123 (45.725%)
Statistics	*P* value*: 0.988			*P* value*: 0.513	
				OR (95% CI): 0.74 (0.52-1.02)	

*, *P*-values are corrected by Bonferroni.

Table 2. Comparison of intraocular pressure between rs76688596 genotypes. *P < 0.05 and **P < 0.01 indicate significant differences compared to the intraocular pressure of the GG group.

rs76688596	Intraocular pressure
GG (342)	17.85 ± 2.34
GC (64)	19.22 ± 2.04*
CC (6)	21.21 ± 2.42**

The GPR97 rs76688596 variant was associated with high IOP in patients with PM

We compared the mean intraocular pressure values of the eyes with more severe phenotypes among different genotypes of PM patients. The results revealed that the intraocular pressure of more affected eyes in PM patients carrying rs76688596 CC (21.21 ± 2.42) was higher than those carrying rs76688596 GG (17.85 ± 2.34, P = 0.007) (Table 2). In addition, the intraocular pressure of the selected affected eye in PM patients with rs76688596 GC (19.22 ± 2.04) was higher compared to those with rs76688596 GG (17.85 ± 2.34, P = 0.037).

GPR97 rs76688596 variant stimulates IOP-related gene expression

We overexpressed GPR97 Gly396 normal protein and GPR97 Arg396 mutant protein in primary HSF cells. All extracted RNA met the quality and integrity criteria for reverse transcription. The quality and efficiency of the RT-PCR results were initially evaluated using melting curves and Ct values. Only Ct values from successful RT-PCR reactions were used for gene expression analysis. RT-PCR results showed that GPR97 Arg396 overexpressing cells significantly up-regulated the mRNA levels of ocular hypertension genes serine/arginine-rich splicing factor 3 (*SFRS3*, 2.56 ± 0.52 folds compared to GPR97 Gly396 group), peptidyl-prolyl cis-trans isomerase 4 (*FKBP4*, 1.61 ± 0.72 folds compared to GPR97 Gly396 group), peptidyl-prolyl cis-trans isomerase 5 (*FKBP5*, 1.18 ± 0.11 folds compared to GPR97 Gly396 group), and nuclear receptor subfamily 3 group C member 1 (*NR3C1*, 1.71 ± 0.31 folds compared to GPR97 Gly396 group) (Fig. 1).

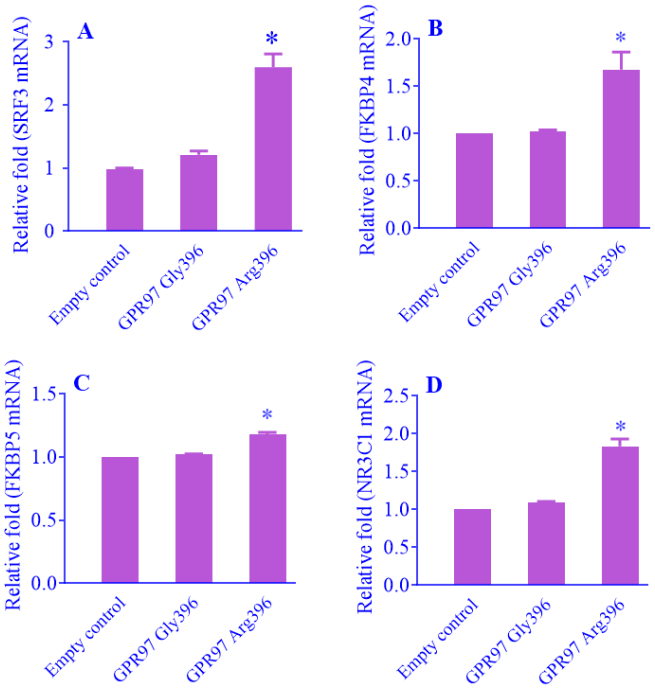

Fig. 1. *GPR97* rs76688596 variant is implicated in elevated intraocular pressure. RT-PCR showed that the mRNA levels of ocular hypertension genes (A-D) SFRS3, FKBP4, FKBP5, and NR3C1 in primary human scleral fibroblast cells after transfection with GPR97 Gly396 WT gene and GPR97 Arg396 mutant gene. Data are representative of at least two independent experiments, mean ± SEM. *P < 0.05 indicates significant differences compared to the control group.

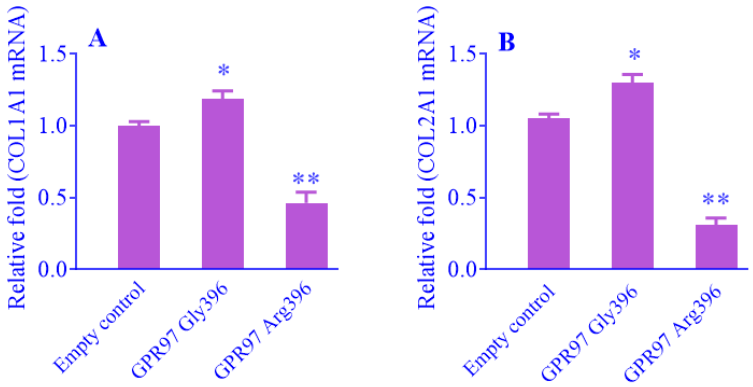

Fig. 2. *GPR97* rs76688596 variant affected COL1A1 and COL2A1 expression. RT-PCR showed that the mRNA levels of (A) COL1A1 and (B) COL2A1 in human scleral fibroblast cells after transfection with GPR97 Gly396 WT gene and GPR97 Arg396 mutant gene. Data are representative of at least two independent experiments, mean ± SEM. **P* < 0.05 and ***P* < 0.01 indicate significant differences compared to the empty vector.

GPR97 rs76688596 variant reduced the expression of COL1A1 and COL2A1

We overexpressed GPR97 Gly396 normal protein and GPR97 Arg396 mutant protein in primary HSF cells. RT-PCR results showed that the mRNA levels of COL1A1 and COL2A1 were significantly down-regulated in GPR97 Arg396 overexpressing cells (Fig. 2A and B: COL1A1, 0.35 ± 0.07 folds compared to GPR97 Gly396 group; COL2A1, 0.23 ± 0.02 folds compared to GPR97 Gly396 group).

GPR97 rs76688596 variant alters N-cadherin and fibronectin expression and reduces cell migration ability

We examined the effects of cortisone stimulation of GPR97 mutants on cell morphology and function. The normal cultured primary HSFs cells and cells induced with were GPR97 WT Gly396 and GPR97 mutant Arg396 shown regularly arranged, growing in monolayer, flat and polygonal, with transparent cytoplasm, round or oval nuclei, distinct nucleoli, and clear borders; After 24 h of 16 nM cortisone stimulation, cellular type was disordered, the cell body became longer and larger, the shape was irregular. We continued to analyze the effect of cortisone on the expression of N-cadherin and fibronectin in HSF cells. Forced expression of the GPR97 Gly396 WT protein in HSF cells did not significantly alter N-cadherin and fibronectin mRNA expression levels compared to the control group. In contrast, overexpression of the GPR97 Arg396 mutant protein in HSF cells significantly decreased N-cadherin mRNA expression and significantly increased fibronectin mRNA expression compared to the control group (Fig. 3A and B). Following 24 h of 16 nM cortisone stimulation, N-cadherin mRNA was significantly inhibited in HSF cells expressing the GPR97 Arg396 mutant protein compared to those expressing the GPR97 WT protein, whereas fibronectin mRNA expression was even higher in the GPR97 Arg396 mutant protein-expressing HSF cells (Fig. 3A and B). These data indicated that the glucocorticoid-GPR97 axis was significantly inhibited by the GPR97 Gly396Arg mutation.

The scratch test results indicated that wound healing in cells expressing GPR97 Gly396 was slower than in the control group (Fig. 3C and Fig. S1), suggesting that the GPR97 WT protein enhances cell adhesion. However, overexpression of the GPR97 Arg396 mutant protein in HSF cells significantly reduced cell healing ability, indicating that the GPR97 Arg396 mutation impairs cell migration. After 24 h of 16 nM cortisone stimulation, cell migration was slower in both GPR97 WT and GPR97 Arg396 expressing cells compared to the vehicle treatment (Fig. 3C). Immunofluorescence staining with phalloidin-FITC and N-cadherin showed that GPR97 Arg396 expression in HSF cells led to the disassembly of actin stress fibers, further indicating that the GPR97 Arg396 mutation reduces cellular migratory ability (Fig. 3D and E).

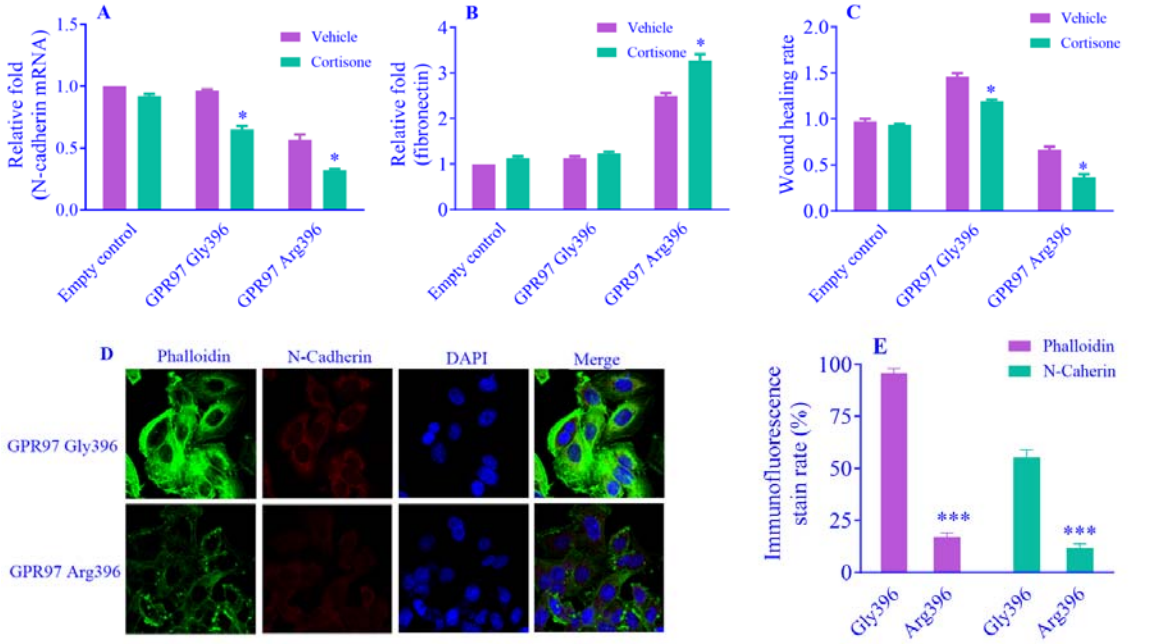

Fig. 3. *GPR97* rs76688596 variant altered N-cadherin and fibronectin mRNA levels and affected cell migration ability. (A and B) RT-PCR showed that the alteration of mRNA levels of N-cadherin and fibronectin in HSF cells after transfection with the GPR97 Gly396 WT gene and the GPR97 Arg396 mutant gene. Cells were stimulated with cortisone (16 nM) for 24 h, and the mRNA level was examined for N-cadherin and fibronectin expression; (C) the scratch test was performed in primary HSF cells transfected with the GPR97 Gly396 WT gene and the GPR97 Arg396 mutant gene. Cells were stimulated with cortisone (16 nM) for 24 h, and the width of the scratch wound was observed and recorded under an optical microscope at 0 h and 24 h of the experiment, respectively. Data are representative of at least two independent experiments, mean ± SEM. **P* < 0.05 and ***P* < 0.01 indicate significant differences compared to the empty vector. (D) Immunofluorescence was performed to measure the disassembly of actin stress fibres by detecting phalloidin-FITC and N-cadherin in the cells expressing GPR97 Gly396 WT protein and GPR97 Arg396 mutant protein. DAPI was used to stain the nuclei as a control. Original view: ×63. (E) Statistical analysis of phalloidin and N-cadherin expression by immunofluorescence between GPR97 Gly396 and GPR97 Arg396 groups. Data represent mean ± SEM from three different experiments. ****P* < 0.001 indicates significant differences in immunofluorescent stain rate between GPR97 Gly396 versus GPR97 Arg396 groups.

Differential glucocorticoid sensitivity influenced by GPR97 genotypes in PM patients receiving oral glucocorticoid treatment

We further investigated the association between the impact of oral corticosteroids on myopia progression and different GPR97 rs76688596 genotypes. For PM patients with the GPR97 rs76688596 GG genotype (n = 12), no significant differences in AL, SE, and IOP were observed at 1- and 3-month post-treatment compared to baseline. However, improvements in BCVA and visual field MS became evident at 3 months. Significant differences were observed when comparing baseline, 1 month, and 3 months with 6-, 12-, 18-, and 24-month post-treatment, as shown in Table 3. For PM patients with the GPR97 rs76688596 GC genotype (n = 13), no significant differences in AL, SE, IOP, and MS were observed at 1- and 3-month post-treatment compared to baseline. BCVA showed no statistical significance at 1 month but exhibited a significant difference at 3 months post-treatment. Similar significant differences were observed when comparing baseline, 1 month, and 3 months with 6-, 12-, 18-, and 24-month post-treatment, as shown in Table 3. In PM patients with the GPR97 rs76688596 CC genotype (n = 6), significant improvements in AL, SE, IOP, BCVA, and MS were observed at 1-month post-treatment compared to baseline (Table 4). Continuous improvements were noted at 3 months post-treatment and further enhancements from 3 to 6 months. Although no significant changes occurred from 6 months to 12 months, indicators remained stable from 12 to 24 months compared to 6 months post-treatment. Comparing 6 months with 12-, 18-, and 24-month post-treatment, IOP continued to decrease significantly, and LogMAR vision showed that BCVA exhibited a significant reduction, as shown in Table 3.

Table 3. Comparison of AL, IOP, SE, BCVA, and MS before and after treatment.

Treatment duration	AL (mm)	IOP (mmHg)	SE	BCVA	MS (dB)
rs76688596, GG (n = 12)					
pre-treatment	29.12 ± 1.22	18.07 ± 2.20	-11.37 ± (-1.44)	0.55 ± 0.17	14.39 ± 1.79
1 month after treatment	29.10 ± 1.55	18.05 ± 1.89	-11.28 ± (-1.41)	0.52 ± 0.16	14.41 ± 1.39
3 months after treatment	29.09 ± 1.38	18.05 ± 2.33	-11.25 ± (-1.33)	0.45 ± 0.15[ab]	14.56 ± 1.54[ab]
6 months after treatment	28.35 ± 1.74[abc]	17.57 ± 1.73[abc]	-11.03 ± (-1.09)[abc]	0.39 ± 0.12[abc]	15.12 ± 1.35[abc]
12 months after treatment	28.45 ± 1.35[abc]	17.07 ± 2.05[abc]	-11.21 ± (-1.11)[abc]	0.32 ± 0.13[abcd]	15.89 ± 1.39[abcd]
18 months after treatment	28.64 ± 1.18[abc]	16.78 ± 1.74[abcd]	-11.22 ± (-1.07)[abc]	0.27 ± 0.11[abcde]	16.39 ± 1.77[abcde]
24 months after treatment	28.69 ± 1.59[abc]	16.39 ± 1.68[abcde]	-11.15 ± (-1.39)[abc]	0.31 ± 0.13[abcd]	15.76 ± 1.62[abcef]
rs76688596, GC (n = 13)					
pre-treatment	29.16 ± 2.98	19.41 ± 2.63	-10.88 ± (-1.12)	0.54 ± 0.19	14.55 ± 2.33
1 month after treatment	29.11 ± 1.77	19.31 ± 1.77	-10.72 ± (-1.25)	0.51 ± 0.18	14.61 ± 1.53
3 months after treatment	29.05 ± 1.98	19.21 ± 1.56	-10.58 ± (-1.54)	0.46 ± 0.17[ab]	14.79 ± 1.77
6 months after treatment	28.16 ± 2.22[abc]	18.41 ± 2.44[abc]	-10.38 ± (-1.47)[ab]	0.39 ± 0.11[abc]	15.55 ± 1.55[ab]
12 months after treatment	28.33 ± 1.77[abc]	17.86 ± 1.32[abcd]	-10.17 ± (-1.24)[abc]	0.33 ± 0.14[abcd]	15.96 ± 1.24[abc]
18 months after treatment	28.55 ± 1.96[abc]	17.52 ± 1.22[abcd]	-10.25 ± (-1.33)[ab]	0.28 ± 0.13[abcde]	16.55 ± 1.39[abcde]
24 months after treatment	28.76 ± 1.99[ab]	17.41 ± 2.11[abcde]	-10.33 ± (-1.09)[ab]	0.29 ± 0.12[abcde]	15.79 ± 2.09[abef]
rs76688596, CC (n = 6)					
pre-treatment	29.23 ± 2.69	21.14 ± 2.30	-11.08 ± (-2.11)	0.54 ± 0.21	14.11 ± 1.49
1 month after treatment	28.89 ± 1.44[a]	19.89 ± 1.55[a]	-10.85 ± (-1.31)[a]	0.46 ± 0.11[a]	15.45 ± 1.35[a]
3 months after treatment	28.79 ± 1.53[ab]	19.77 ± 1.63[ab]	-10.78 ± (-1.52)[ab]	0.44 ± 0.14[ab]	15.33 ± 1.23[ab]
6 months after treatment	28.19 ± 1.67[abc]	18.21 ± 1.87[abc]	-10.06 ± (-1.39)[abc]	0.36 ± 0.11[abc]	16.22 ± 1.35[abc]
12 months after treatment	28.23 ± 1.68[abc]	17.71 ± 2.14[abcd]	-10.08 ± (-2.15)[abc]	0.30 ± 0.13[abcd]	16.77 ± 1.63[abc]
18 months after treatment	28.15 ± 1.51[abc]	17.04 ± 2.01[abcde]	-10.34 ± (-1.77)[abc]	0.28 ± 0.12[abcd]	16.12 ± 1.36[abc]
24 months after treatment	28.14 ± 1.63[abc]	17.15 ± 1.94[abcde]	-10.32 ± (-1.98)[abc]	0.29 ± 0.12[abcd]	15.78 ± 1.68[abde]

[a]$P < 0.05$, In comparison to pre-treatment, [b]$P < 0.05$ versus 1-month post-treatment, [c]$P < 0.05$ versus 3 months post-treatment, [d]$P < 0.05$ versus 6 months post-treatment, [e]$P < 0.05$ versus12 months post-treatment, and [f]$P < 0.05$ versus 18 months post-treatment; AL, Axial length; IOP, intraocular pressure; SE, spherical equivalent; BCVA, best-corrected visual acuity; MS, mean sensitivity

Table 4. Correlation analysis of AL with IOP and SE at each time point after treatment.

Treatment	AL and IOP	AL and SE
rs76688596, GG (12)		
1 month	0.021	-0.027
3 months	0.033	-0.054
6 months	0.521*	-0.217*
12 months	0.412*	-0.189*
18 months	0.238*	-0.298*
24 months	0.127*	-0.117*
rs76688596, GC (13)		
1 month	0.017	-0.054
3 months	0.058	-0.037
6 months	0.278*	-0.143*
12 months	0.387**	-0.217**
18 months	0.474*	-0.321*
24 months	0.127*	-0.254*
rs76688596, CC (6)		
1 month	0.124*	-0.113*
3 months	0.158*	-0.152*
6 months	0.237**	-0.167*
12 months	0.387**	-0.137**
18 months	0.457**	-0.159**
24 months	0.498**	-0.257**

AL, Axial length; IOP, intraocular pressure; SE, spherical equivalent. *$P < 0.05$ and **$P < 0.01$ values were calculated to assess correlations between AL and IOP and between AL and SE in rs76688596 GG, GC, and CC groups at each post-treatment time point.

Correlation analysis of AL with IOP and SE at each time point after treatment

In PM patients carrying the GPR97 rs76688596 GG genotype (n = 12), we conducted a correlation analysis of AL with IOP and SE at various time points post-treatment. We observed no correlation between AL, IOP, and SE at 1- and 3-month post-treatment. However, at 6-, 12-, 18-, and 24-month post-treatment, AL showed a positive correlation with IOP and a negative correlation with SE (Table 4). For PM patients carrying the GPR97 rs76688596 GC genotype (n = 13), a similar correlation analysis was performed at different time points post-treatment. Similar to the GG genotype group, no correlation was observed between AL, IOP, and SE at 1- and 3-month post-treatment. Nevertheless, at 6-, 12-, 18-, and 24-month post-treatment, AL exhibited a positive correlation with IOP and a negative correlation with SE (Table 4). In PM patients carrying the GPR97 rs76688596 CC genotype (n = 12), a correlation analysis of AL with IOP and SE was conducted at various time points post-treatment. In contrast to the other genotypes, significant correlations were observed at 1-, 3-, 6-, 12-, 18-, and 24-month post-treatment, where AL positively correlated with IOP and negatively correlated with SE (Table 4).

DISCUSSION

Our study identified the involvement of GPR97 in axial elongation, contributing to the PM mutation database and opening new therapeutic possibilities. Specifically, targeting the glucocorticoid-GPR97 interaction within the eye could inhibit ocular elongation, providing a novel approach to prevent the progression of myopic maculopathy and optic nerve damage. Our findings align with previous studies showing that *in vivo* regulation of multiple signalling pathways plays a critical role in myopia development by influencing protein expression and matrix remodeling in the posterior sclera (19-23). Consistent with these studies (21,24), we observed a significant reduction in type I collagen expression, a key component of the scleral extracellular matrix, in PM compared to normal eyes. Notably, collagen type I levels were lower in the posterior pole than in the anterior pole of normal eyes, indicating region-specific collagen distribution associated with PM development. Our study demonstrated that the GPR97 rs76688596 variant specifically downregulated COL1A1 and COL2A1 expression, which may contribute to altered collagen synthesis and matrix remodeling in PM. This variability in findings could also result from differences in glucocorticoid exposure and individual genetic backgrounds, as glucocorticoid responses are known to be highly individualized due to genetic polymorphisms. Further research is needed to explore additional genetic loci and regulatory factors that modulate type I collagen expression in PM. Such insights could advance our understanding of PM pathogenesis and support the development of targeted therapies, particularly by modulating the glucocorticoid-GPR97 axis.

Our study demonstrated that the GPR97 Arg396 variant upregulated ocular hypertension-related genes, including *SFRS3, FKBP4, FKBP5,*

and *NR3C1* (Fig. 1), suggesting a significant impact of the GPR97 Gly396Arg mutation on the glucocorticoid-GPR97 axis. Consistent with recent findings by Ping *et al*. (10), who revealed distinct GPR97 activation mechanisms *via* single-particle cryo-electron microscopy, our results support the role of GPR97 in modulating cellular processes such as cytoskeletal rearrangement, cell adhesion, and migration through small GTPase regulation (11). These studies highlighted the unique glucocorticoid binding to GPR97 through hydrophobic interactions and hydrogen bonding, differing from other GPCR family receptors due to the absence of conserved motifs (10). In our scratch test, cells expressing the GPR97 Gly396 variant exhibited slower wound healing at the 24-h mark compared to controls (Fig. 3), aligning with previous reports that normal GPR97 enhances cell adhesion (11). The overexpression of the GPR97 Arg396 mutant protein in human scleral fibroblasts further reduced cell migration, underscoring the mutation's role in impairing cell healing ability. Additionally, Go palmitoylation, which enhances GPR97-Go interaction and stabilizes the ligand-binding cavity (12), may be disrupted by mutations in GPR97-interacting amino acids, such as Gly396Arg. This disruption could affect key cellular functions, contributing to PM. The significance of our work lies in establishing GPR97 as a critical functional candidate gene in PM, with its dysregulation contributing to altered collagen expression and impaired adhesion in the sclera and retinal epithelium. Further research is needed to explore the broader implications of the glucocorticoid-GPR97 axis in PM development.

PM is characterized by excessive AL growth, leading to structural changes in the retina, choroid, and sclera, and ultimately causing severe visual impairments (13). The elongation of AL, a hallmark of PM, correlates with changes in refractive error. Glucocorticoids, steroid hormones produced by the adrenal cortex (16), act through glucocorticoid receptors to regulate gene expression (15,25). However, prolonged glucocorticoid use may increase IOP and risk of glaucoma and cataracts, primarily due to enhanced resistance in aqueous humor outflow pathways (14-17). Genetic factors, including MYOC and IGFBP2, influence the IOP response to glucocorticoids. Our study demonstrated that glucocorticoid use in the eye, whether local or systemic, could elevate IOP and contribute to hormonal glaucoma (26). Scleral hypoxia, often from chronic choroidal inflammation, activates receptor-mediated signaling that accelerates myopia progression (27). Inflammatory cytokines, such as IL-6 and TNF-α, further drive myopia development under inflammatory conditions (28). Corticosteroids like oral prednisone, used for inflammatory choroidal diseases, modulate these inflammatory mediators. Due to the risks of high-dose corticosteroid therapy, our study applied a moderate-dose regimen with a gradual taper to manage PM progression, focusing on controlling AL, refractive error (SE), and preserving visual function. By reducing IOP, our treatment aimed to limit scleral expansion, slow scleral degradation, inhibit fibroblast activation, enhance choroidal blood flow, and reduce scleral ischemia and hypoxia (29). Our findings revealed genotype-specific responses to glucocorticoid therapy. Patients with the GPR97 rs76688596 GG genotype showed no significant changes in AL, SE, or IOP at 1- and 3-month post-treatment, though improvements in BCVA and visual field mean sensitivity emerged after 3 months. The GPR97 rs76688596 GC genotype group exhibited a delayed yet similar response. In contrast, patients with the GPR97 rs76688596 CC genotype displayed a rapid and sustained improvement across all parameters, including AL, SE, IOP, BCVA, and visual field mean sensitivity, starting as early as 1-month post-treatment and persisting throughout the 24-month follow-up. These genotype-specific responses suggest a critical role of the *GPR97* rs76688596 variant in influencing glucocorticoid treatment efficacy in PM, highlighting the potential for personalized therapeutic strategies tailored to genetic profiles.

Limitations of this study include several factors. We selected patients with diopters higher than -6.0 D as our criteria, yet not all may accurately represent pathological myopia. Additionally, significant genetic diversity across different racial groups suggests that our findings require validation in larger, independent cohorts. Moreover, factors like study duration, seasonal variations, ambient lighting, and the volume of near work

performed could be potential confounders. Also, environmental and lifestyle factors, such as age, duration of corticosteroid use, and concurrent medications, may act as confounders in the observed genetic influence on corticosteroid response. Finally, to fully explore the *in vivo* role of GPR97 in high myopia development, future studies should consider employing GPR97 knockout animal models such as Danio rerio or rodent models.

CONCLUSION

In this study, we identified a significant association between the *GPR97* rs76688596 variant and PM. Patients with the CC genotype exhibited elevated intraocular pressure, highlighting GPR97's role in PM susceptibility. Mechanistically, *GPR97* rs76688596 influences the glucocorticoid-GPR97 axis, altering N-cadherin and fibronectin expression and reducing primary scleral fibroblast cell migration. These findings provide crucial insights into high myopia's pathogenesis. Additionally, our study revealed varied responses to oral glucocorticoids for reducing intraocular pressure based on GPR97 genotypes, emphasizing the potential of personalized medicine in effectively managing PM progression. This underscores the importance of considering GPR97 genetic susceptibility in treatment response and PM management strategies.

Acknowledgements

This study was financially supported by the Zhangjiagang City Science and Technology through the Plan Project: ZKY202127.

Conflicts of interest statements

All authors declared no conflict of interest in this study.

Author contributions

L. Pu, G. Wu, Q. Zhao, Z. Mu, and Y. Xu contributed to the conceptualization, methodology, and investigation; Q. Zhao, L. Pu, and G. Wu wrote the first draft of the manuscript; Q. Zhao, Y. Xu, L. Pu, Z. Mu, and W. Cheng were responsible for specimen collection and acquisition of clinical data. All authors have read and approved the finalized article. Each author has fulfilled the authorship criteria and affirmed that this article represents honest and original work.

Availability of data and material

All data generated or analyzed during this study are included in this article. Further enquiries can be directed to the corresponding author.

Consent to participate

Written informed consent was obtained from all participants or their parent/legal guardian/next of kin before study participation.

Consent for publication

All named authors meet the ICMJE criteria for authorship for this article, take full responsibility for the integrity of the work as a whole, and have given their approval for this version to be published.

AI declaration

The authors did not use any AI-assisted technologies in the preparation of this manuscript.

Supplementary material

The supplementary illustrations are available online at https://github.com/lijunpu147/myopia-genetics-study.

REFERENCES

1. Ohno-Matsui K, Wu PC, Yamashiro K, Vutipongsatorn K, Fang Y, Cheung CMG, *et al*. IMI pathologic myopia. Invest Ophthalmol Vis Sci. 2021;62(5):5,1-36. DOI: 10.1167/iovs.62.5.5.
2. Chu R, Ni P, Ni M, Shen F. Genetic epidemiology study of pathological myopia. Chin J Med Gen. 2000;17(3):178-180. PMID: 10837519.
3. Zhu G, Hewitt AW, Ruddle JB, Kearns LS, Brown SA, Mackinnon JR, *et al*. Genetic dissection of myopia: evidence for linkage of ocular axial length to chromosome 5q. Ophthalmology. 2008;115(6):1053-1057. DOI: 10.1016/j.ophtha.2007.08.013.
4. Ratnamala U, Lyle R, Rawal R, Singh R, Vishnupriya S, Himabindu P, *et al*. Refinement of the X-linked nonsyndromic high-grade myopia locus MYP1 on Xq28 and exclusion of 13 known positional candidate genes by direct sequencing. Invest Ophthalmol Vis Sci. 2011;52(9):6814-6819. DOI: 10.1167/iovs.10-6815.

5. Zhao YY, Zhang FJ, Zhu SQ, Duan H, Li Y, Zhou ZJ, *et al*. The association of a single nucleotide polymorphism in the promoter region of the LAMA1 gene with susceptibility to Chinese high myopia. Mol Visi. 2011;17:1003-1010. PMID: 21541277.
6. Deng ZJ, Shi KQ, Song YJ, Fang YX, Wu J, Li G, *et al*. Association between a lumican promoter polymorphism and high myopia in the Chinese population: a meta-analysis of case-control studies. Ophthalmologica. 2014;232(2):110-117. DOI: 10.1159/000356698.
7. Siwko S, Lai L, Weng J, Liu M. Lgr4 in ocular development and glaucoma. J Ophthalmol. 2013;2013:987494,1-9. DOI: 10.1155/2013/987494.
8. Reyes-Resina I, Awad Alkozi H, Del Ser-Badia A, Sanchez-Naves J, Lillo J, Jimenez J, *et al*. Expression of melatonin and dopamine D3 receptor heteromers in eye ciliary body epithelial cells and negative correlation with ocular hypertension. Cells. 2020;9(1):152,1-20. DOI: 10.3390/cells9010152.
9. Patel N, Itakura T, Gonzalez Jr, Schwartz SG, Fini ME. GPR158, an orphan member of G protein-coupled receptor Family C: glucocorticoid-stimulated expression and novel nuclear role. PLoS One. 2013;8(2):e57843,1-16. DOI: 10.1371/journal.pone.0057843.
10. Ping YQ, Mao C, Xiao P, Zhao RJ, Jiang Y, Yang Z, *et al*. Structures of the glucocorticoid-bound adhesion receptor GPR97-Go complex. Nature. 2021;589(7843):620-626. DOI: 10.1038/s41586-020-03083-w.
11. Valtcheva N, Primorac A, Jurisic G, Hollmen M, Detmar M. The orphan adhesion G protein-coupled receptor GPR97 regulates migration of lymphatic endothelial cells via the small GTPases RhoA and Cdc42. J Biol Chem. 2013;288(50):35736-35748. DOI: 10.1074/jbc.M113.512954.
12. Zhang H, Chu G, Wang G, Yao M, Lu S, Chen T. Mechanistic understanding of the palmitoylation of G(o) protein in the allosteric regulation of adhesion receptor GPR97. Pharmaceutics. 2022;14(9):1-16. DOI: 10.3390/pharmaceutics14091856.
13. Wei WB, Dong L. Paying attention to the fundus complications and improving the prevention and treatment of pathological myopia. Chin J Ophthalmol. 2021;57(6):401-405. DOI: 10.3760/cma.j.cn112142-20210114-00035.
14. Bermudez JY, Webber HC, Brown B, Braun TA, Clark AF, Mao W. A Comparison of gene expression profiles between glucocorticoid responder and non-responder bovine trabecular meshwork cells using RNA sequencing. PLoS One. 2017;12(1):e0169671,1-20. DOI: 10.1371/journal.pone.0169671.
15. Rufer F, Uthoff D. [Symptoms and therapy for steroid glaucoma]. Klin Monbl Augenheilkd. 2013;230(7):692-696. DOI: 10.1055/s-0032-1328472.
16. Urban RC Jr, Dreyer EB. Corticosteroid-induced glaucoma. Int Ophthalmol Clin. 1993;33(2):135-139. DOI: 10.1097/00004397-199303320-00013.
17. Zode GS, Sharma AB, Lin X, Searby CC, Bugge K, Kim GH, *et al*. Ocular-specific ER stress reduction rescues glaucoma in murine glucocorticoid-induced glaucoma. J Clin Invest. 2014;124(5):1956-1965. DOI: 10.1172/JCI69774.
18. Qiu C, Chen M, Yao J, Sun X, Xu J, Zhang R, *et al*. Mechanical strain induces distinct human scleral fibroblast lineages: differential roles in cell proliferation, apoptosis, migration, and differentiation. Invest Ophthalmol Vis Sci. 2018;59(6):2401-2410. DOI: 10.1167/iovs.18-23855.
19. Gentle A, Liu Y, Martin JE, Conti GL, McBrien NA. Collagen gene expression and the altered accumulation of scleral collagen during the development of high myopia. J Biol Chem. 2003;278(19):16587-16594. DOI: 10.1074/jbc.M300970200.
20. Lam DS, Lee WS, Leung YF, Tam PO, Fan DS, Fan BJ, *et al*. TGFbeta-induced factor: a candidate gene for high myopia. Invest Ophthalmol Vis Sci. 2003;44(3):1012-1015. DOI: 10.1167/iovs.02-0058.
21. Inamori Y, Ota M, Inoko H, Okada E, Nishizaki R, Shiota T, *et al*. The COL1A1 gene and high myopia susceptibility in Japanese. Hum Genet. 2007;122(2):151-157. DOI: 10.1007/s00439-007-0388-1.
22. Harper AR, Summers JA. The dynamic sclera: extracellular matrix remodeling in normal ocular growth and myopia development. Exp Eye Res. 2015;133:100-111. DOI: 10.1016/j.exer.2014.07.015.
23. Li M, Luo Z, Yan X, Chen Z. The anterior segment biometrics in high myopia eyes. Ophthalmic Res. 2023;66(1):75-85. DOI: 10.1159/000526280.
24. Metlapally R, Li YJ, Tran-Viet KN, Abbott D, Czaja GR, Malecaze F, *et al*. COL1A1 and COL2A1 genes and myopia susceptibility: evidence of association and suggestive linkage to the COL2A1 locus. Invest Ophthalmol Vis Sci. 2009;50(9):4080-4086. DOI: 10.1167/iovs.08-3346.
25. Dibas A, Yorio T. Glucocorticoid therapy and ocular hypertension. Eur J Pharmacol. 2016;787:57-71. DOI: 10.1016/j.ejphar.2016.06.018.
26. Wang XQ, Duan ZX, He XG, Zhou XY. Clinical relevance of the glucocorticoid receptor gene polymorphisms in glucocorticoid-induced ocular hypertension and primary open angle glaucoma. Int J Ophthalmol. 2015;8(1):169-173. DOI: 10.3980/j.issn.2222-3959.2015.01.30.
27. Zhou X, Ye C, Wang X, Zhou W, Reinach P, Qu J. Choroidal blood perfusion as a potential "rapid predictive index" for myopia development and progression. Eye Vis. 2021;8(1):1,1-5. DOI: 10.1186/s40662-020-00224-0.
28. Chen W, Zhao B, Jiang R, Zhang R, Wang Y, Wu H, *et al*. Cytokine expression profile in aqueous humor and sera of patients with acute anterior uveitis. Curr Mol Med. 2015;15(6):543-549. DOI: 10.2174/1566524015666150731100012.
29. Wang P, Chen S, Liu Y, Lin F, Song Y, Li T, *et al*. Lowering intraocular pressure: a potential approach for controlling high myopia progression. Invest Ophthalmol Vis Sci. 2021;62(14):17,1-6. DOI: 10.1167/iovs.62.14.17.